1-1-2014

Giant electrocaloric effect in BaZr0.2Ti0.8O3 thick film

Hui-Jian Ye
Pennsylvania State University

Xiaoshi Qian
Pennsylvania State University

Dae Yong Jeong
Inha University

Shujun Zhang
Pennsylvania State University, shujun@uow.edu.au

Yue Zhou
Pennsylvania State University

See next page for additional authors

Giant electrocaloric effect in BaZr0.2Ti0.8O3 thick film

Abstract

We report the giant electrocaloric effect (ECE) of BaZr0.2Ti0.8O3 (BZT) thick film near room temperature. The BZT thick film was fabricated by the tape casting method with the thickness of 12.0 μm. Due to the near invariant critical point composition, relaxor behavior, and the stress generated between the film and the substrate, the thick film exhibits a large adiabatic temperature drop ΔT = −7 °C under 19.5 MV/m electric field, large EC coefficient ΔT/ΔE = 0.50 x 10−6 K · m · V−1, ΔS/ΔE = 0.88 x 10−6 J · m · kg−1 · K−1 · V−1 over a wide temperature range near room temperature, where ΔS is the isothermal entropy change and ΔE is the applied field. These high EC properties and possibility of fabrication of the EC ceramics into multilayer ceramic capacitor configuration provide solution for the application of the EC material for practical cooling device applications.

Disciplines

Engineering | Physical Sciences and Mathematics

Publication Details

Ye, H., Qian, X., Jeong, D., Zhang, S., Zhou, Y., Shao, W., Zhen, L. & Zhang, Q. (2014). Giant electrocaloric effect in BaZr0.2Ti0.8O3 thick film. Applied Physics Letters, 105 (15), 152908-1-152908-4.

Authors

Hui-Jian Ye, Xiaoshi Qian, Dae Yong Jeong, Shujun Zhang, Yue Zhou, Wen-Zhu Shao, Liang Zhen, and Q M. Zhang

Giant electrocaloric effect in $BaZr_{0.2}Ti_{0.8}O_3$ thick film

Hui-Jian Ye, Xiao-Shi Qian, Dae-Yong Jeong, Shujun Zhang, Yue Zhou, Wen-Zhu Shao, Liang Zhen, and Q. M. Zhang

Citation: Appl. Phys. Lett. **105**, 152908 (2014); doi: 10.1063/1.4898599
View online: https://doi.org/10.1063/1.4898599
View Table of Contents: http://aip.scitation.org/toc/apl/105/15
Published by the American Institute of Physics

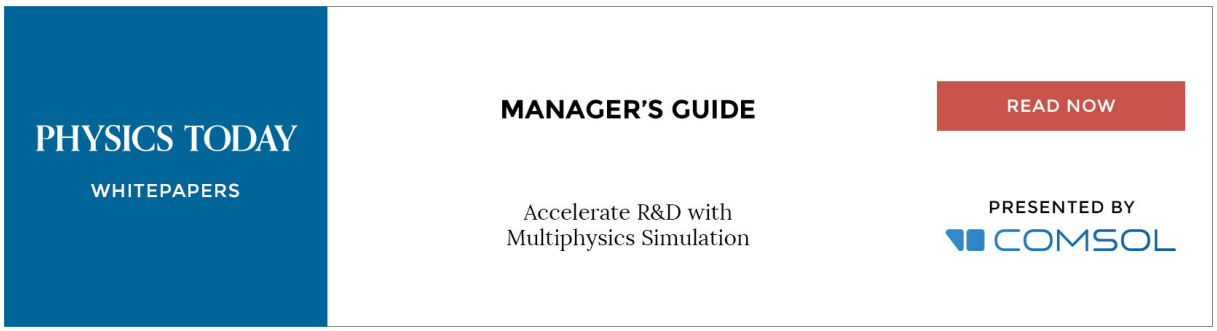

Giant electrocaloric effect in $BaZr_{0.2}Ti_{0.8}O_3$ thick film

Hui-Jian Ye,[1,2] Xiao-Shi Qian,[3] Dae-Yong Jeong,[4] Shujun Zhang,[1] Yue Zhou,[3] Wen-Zhu Shao,[2] Liang Zhen,[2] and Q. M. Zhang[1,3,a)]

[1]*Materials Research Institute, The Pennsylvania State University, University Park, Pennsylvania 16802, USA*
[2]*School of Materials Science and Engineering, Harbin Institute of Technology, Harbin 150001, China*
[3]*Department of Electrical Engineering, The Pennsylvania State University, University Park, Pennsylvania 16802, USA*
[4]*Department of Materials Science and Engineering, Inha University, Incheon 402-751, South Korea*

(Received 25 August 2014; accepted 7 October 2014; published online 17 October 2014)

We report the giant electrocaloric effect (ECE) of $BaZr_{0.2}Ti_{0.8}O_3$ (BZT) thick film near room temperature. The BZT thick film was fabricated by the tape casting method with the thickness of 12.0 μm. Due to the near invariant critical point composition, relaxor behavior, and the stress generated between the film and the substrate, the thick film exhibits a large adiabatic temperature drop $\Delta T = -7\,^{\circ}C$ under 19.5 MV/m electric field, large EC coefficient $\Delta T/\Delta E = 0.50 \times 10^{-6}$ $K \cdot m \cdot V^{-1}$, $\Delta S/\Delta E = 0.88 \times 10^{-6}$ $J \cdot m \cdot kg^{-1} \cdot K^{-1} \cdot V^{-1}$ over a wide temperature range near room temperature, where ΔS is the isothermal entropy change and ΔE is the applied field. These high EC properties and possibility of fabrication of the EC ceramics into multilayer ceramic capacitor configuration provide solution for the application of the EC material for practical cooling device applications. © *2014 AIP Publishing LLC*. [http://dx.doi.org/10.1063/1.4898599]

Electrocaloric effect (ECE), which is induced by the change of entropy in the electric insulators, attracts a lot of concern from fundamental research for engineering applications.[1–4] It may provide a promising method to promote solid state cooling devices for expansive applications from cooling devices in wide range of scales to temperature regulations for the small modern electronics.[5–8] Until recently, large ECE in the polymer, liquid crystal and ceramic materials including thin films and bulk were reported, a big step to realize the advanced cooling device.[9–13] Such as the huge temperature drop, up to 35 °C, was produced in a high energy electron irradiated P(VDF-TrFE) relaxor polymer under 180 MV/m. The ECE of barium titanate has been investigated in past several years in bulk ceramic, films, and single crystal.[17–21] Ferroelectric $BaTiO_3$ thick film with temperature drop about 7.1 °C was observed under the high electric field of 80 MV/m.[14] In the modified $BaTiO_3$ ceramic system, the $Ba(Zr_{0.2}Ti_{0.8})O_3$ (BZT) bulk ceramic showed giant ECE, i.e., large temperature drop about 4.5 °C and large entropy change ($\Delta S = 8\,J \cdot kg^{-1} \cdot K^{-1}$) under 14 MV/m due to the existing invariant critical point, where four different phases, including cubic, tetragonal, orthorhombic, and rhombohedral phases coexist.[15] Also an adiabatic temperature change around 5.3 °C under 90 MV/m at 39 °C was found in the liquid crystal near its nematic–isotropic phase transition.[16] However, larger ECE and EC coefficient are required to compete with the existing cooling system.

Nevertheless, aside of ECE itself, some realistic issues should be considered to realize the EC materials as the solid-state refrigerant devices. For example, the operating voltage should be as low as possible and meanwhile EC material could yield large temperature drop under low voltage. Furthermore, EC coefficient of dielectric is a key parameter in the practical refrigerant cycle. In the previous researches, the EC material exhibits high EC coefficient at low electric field but becomes lower at higher field. Therefore, it is extremely critical to develop the ideal EC materials, which possess large ΔT under low operating voltage (<200 V) and also high EC coefficient over a wide operation temperature range around room temperature.

Considering the above concerns, we fabricated the BZT thick film by tape casting and investigated the EC properties. As reported before, the bulk BZT composition showed a large temperature drop. It was expected that smaller thickness than that of bulk, which corresponds to high ΔE, could yield larger ΔT at the certain voltage. Besides, the more metallic electrode between ceramic thick films would enable the heat to flow more easily.

The BZT thick film was prepared by tape casting method, which is followed by the structure schematic shown in Fig. 1(a). In order to decrease the sintering temperature of

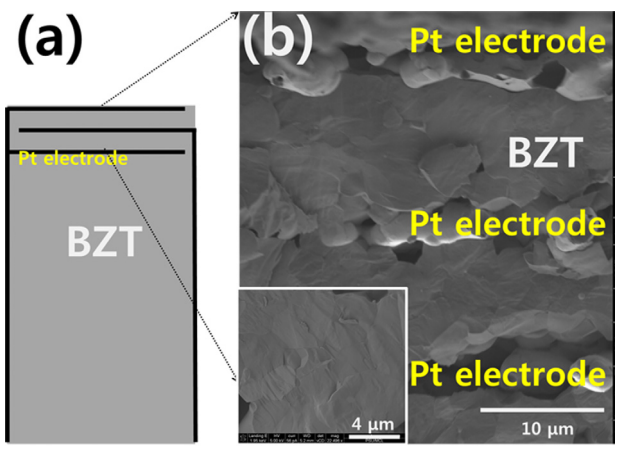

FIG. 1. (a) A schematic of ceramic capacitor architecture and (b) cross-section SEM image of BZT thick films.

a)Author to whom correspondence should be addressed. Electronic mail: qxz1@psu.edu

BZT to below 1200 °C, sinter aids were added in the system. All the chemicals of barium carbonate ($BaCO_3$, 99.8%, 1 μm), zirconium dioxide (ZrO_2, 99.5%, 1 μm), and titanium dioxide (TiO_2, 99.5%, 1–2 μm) were purchased from Alfa Aesar and used directly. Stoichiometric weights of all the powder were mixed with ethanol and milled by zirconia balls for 24 h. After the calcination performed at 1100 °C for 2 h, 0.5 mol. % MnO_2, 1 wt. % polyvinyl alcohol (PVA) binder solution and 1 wt. % sinter aids (PbO and B_2O_3) were added in and then used to fabricate thick films via tape casting. The BZT films with printed Pt electrode were stacked layer by layer with precise alignment during the isostatic lamination. After sintering at 1200 °C in air for 1.5 h, silver paste was used to terminate the opposite ends and forms outer electrode for the further electric characterization.

Temperature dependence of dielectric constant and loss under different frequencies was characterized by HP 4980A LCR meter equipped with a temperature-controlled chamber (Delta 9023). Polarization (P)-electric field (E) loops were measured with Sawyer-Tower circuit as a function of electric field and test temperature. The cross-section image of BZT multilayer films with two active layers is shown in Fig. 1(b) examined by scanning electron microscopy (SEM) (FEI NanoSEM 630). The thickness of single layer is around 12 μm. The heat Q generated and absorbed by the BZT samples was collected by the modified differential scanning calorimetry (DSC) (TA Q2000) to further calculate the temperature drop as a result of ECE. In this set-up, sample was connected with two surface-insulated silver wire electrodes and a power supplier/amplifier (Trek 610C) was used to apply electric field. The input voltage ramp is designed by an arbitrary function generator and is amplified by the Trek. Voltage ramps with constant rate were applied on the sample

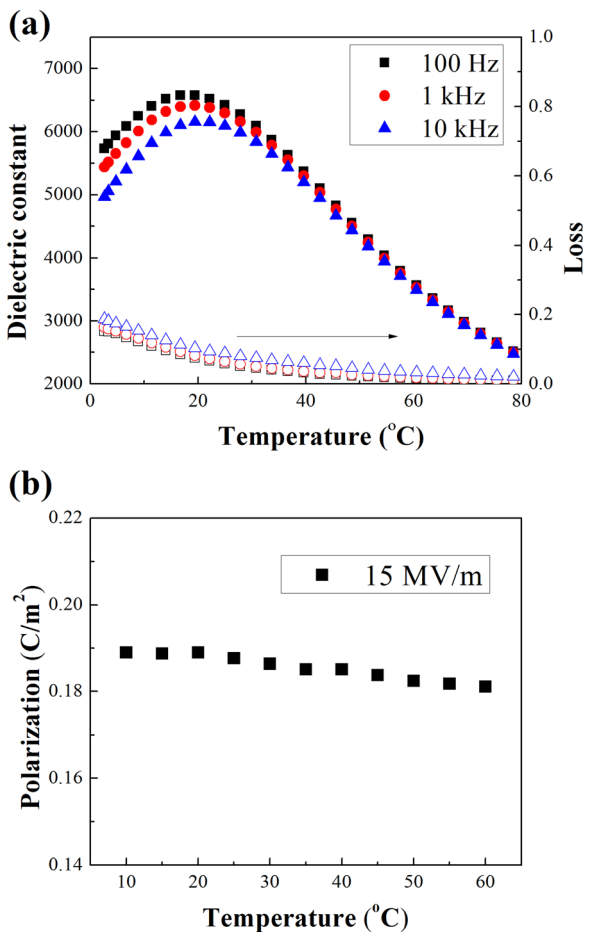

FIG. 2. (a) The dielectric constant and loss of BZT thick film for the temperature change and (b) polarization as a function of temperature for BZT thick film under 15 MV/m.

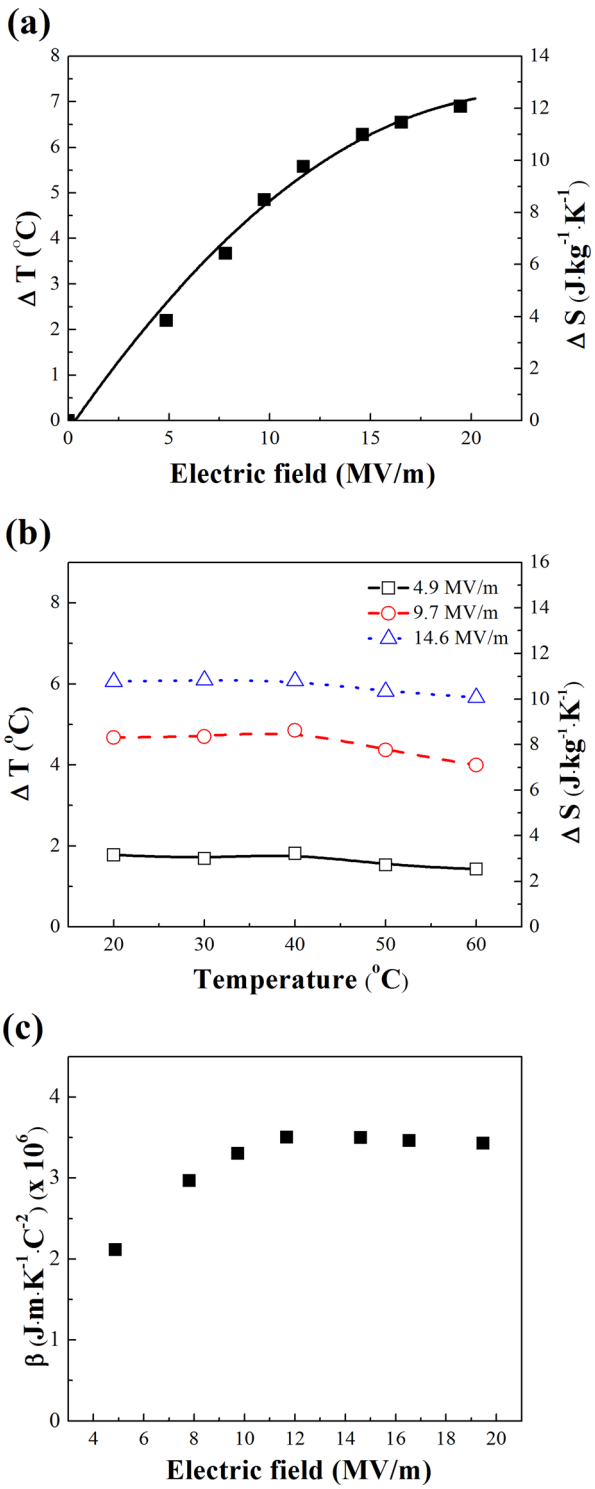

FIG. 3. (a) EC-induced temperature drop ΔT and isothermal entropy change ΔS for the different electric fields at 40 °C. (b) EC-induced temperature drop ΔT and isothermal entropy change ΔS for the temperature changes under different electric fields. (c) β coefficient for the electric fields change at 40 °C. Solid, dashed, and dotted curves are drawn to guide eyes.

during the whole test. The heat capacity of the BZT thick film was also obtained by the DSC.

The temperature dependence of dielectric constant and loss under different frequencies is displayed in Fig. 2(a). The BZT thick film exhibits the relaxor behavior and shows maximum dielectric constant of around 6500 at 20 °C maintaining high value over a wide temperature range. From the inset of Fig. 1(b), the grain size of BZT is 2 to 3 μm, which is smaller than that of bulk ceramic, and the phenomenon of small grain size was attributed to the lower sintering temperature. The polarization of the BZT thick film obtained at 10 Hz as function of test temperature is displayed in Fig. 2(b). The polarization of the BZT thick film reaches 0.19 C/m^2 at 15 MV/m under room temperature. The induced polarization decreases slightly with increasing temperature from 10 to 60 °C and exhibits no obvious peak in the test temperature range, which is consistent with the relaxor nature of the ceramic material.[15]

The heat Q generated and absorbed by the BZT samples was collected with the modified DSC to further calculate the temperature drop as a result of ECE. The isothermal entropy change ΔS can be obtained from $Q = T\Delta S$ and the adiabatic temperature ΔT from $-T\Delta S = c\Delta T$. As shown in Fig. 3(a), a ΔT of 6.3 °C and ΔS of 11.0 J · kg^{-1} · K^{-1} are induced under 14.6 MV/m electric field change at 40 °C, which is higher than those of bulk BZT ceramic under the same environment. The maximum $\Delta T = 7.0$ °C is obtained under 19.5 MV/m for the thick film in our study. As shown in Fig. 3(b), ΔT and ΔS are nearly constant over a broad range from 20 to 60 °C.

In order to quantify the efficiency of ECE, according to the thermodynamic phenomenological theory, Gibbs free energy can be expanded in terms of polarization P

$$G = \frac{1}{2}\alpha P^2 + \frac{1}{2}\xi P^4 + \frac{1}{2}\gamma P^6, \tag{1}$$

where $\alpha = \beta(T - T_0)$, where β is a coefficient. From $\left(\frac{\partial G}{\partial T}\right)_D = -\Delta S$, it is derived as $\Delta S = -\beta P^2/2$, i.e., ΔS is proportional to the square of the polarization. Besides, applying the following equation $-T\Delta S = c\Delta T$ yields the adiabatic temperature change $\Delta T = \beta T D^2/2c$, where c is the specific heat capacity.[28] Applying the data of polarization and ECE of samples, the β values of BZT thick film are shown in Fig. 3(c). The value of β is 3.5×10^6 J · m · K^{-1} · C^{-2} at 11.7 MV/m, which is much higher than that of bulk ceramic (less than 3.0×10^6 J · m · K^{-1} · C^{-2}). Also the EC coefficient of BZT thick film is larger, $\Delta T/\Delta E = 0.50 \times 10^{-6}$ K · m · V^{-1} and $\Delta S/\Delta E = 0.88 \times 10^{-6}$ J · m · kg^{-1} · K^{-1} · V^{-1} at 9.8 MV/m, respectively. Table I presents some reported ECE properties of $BaTiO_3$ and modified ceramics from bulk to film. The temperature change of thin film and single crystal is also included to compare. It can be observed that the BZT thick film in this work exhibits great ECE performance, such as high temperature drop ΔT, large $\Delta T/\Delta E$, $\Delta S/\Delta E$, and especially large β even under high ΔE, which could provide solution for the application of EC material in the practical cooling device.

This enhancement of ECE property is explained with the combination of invariant critical point and ferroelectric relaxor behavior around room temperature. In this study, two active layers were prepared on the same composition films substrate. Therefore, the stress is generated between the thick film and the BZT substrate during applying and removing of electric field, which is another field to increase the coexisting phases and further giant ECE of material is obtained. The internal stress resulted from the mechanical constraint of the substrate plays an important role in the enhanced ECE of ferroelectric thick film. The EC effect, which is driven by electric field and generated near invariant critical points with different coexisting phases, could be tuned by the second kind of field, the stress. Giant temperature drop can be observed due to stress, even creates a phase transition in the ferroelectric system.[29,30] The total pyroelectric coefficient measured at constant stress p^X can be expressed as[31–33]

$$p_i^X = p_i^x + d_{ijk}{}^X c_{jklm}{}^{X,E} \alpha_{lm}{}^E, \tag{2}$$

where $d_{ijk}{}^X$ is the piezoelectric strain tensor under a constant stress, $c_{jklm}{}^{X,E}$ is the elastic stiffness tensor under constant stress and electric field, and $\alpha_{lm}{}^E$ is the thermal expansion tensor under a constant. The second term in the equation is

TABLE I. Comparison of EC properties of BZT developed here with those in the literature.

Material	Form	T (°C)	ΔT (K)	ΔE (MV/m)	$\Delta T/\Delta E$ (10^{-6} K · m · V^{-1})	$\Delta S/\Delta E$ (10^{-6} J · m · kg^{-1} · K^{-1} · V^{-1})	β (10^6 J · m · K^{-1} · C^{-2})	Method	References
$BaZr_{0.2}Ti_{0.8}O_3$	Thick film	40	4.9	9.7	0.51	0.88	3.4	DSC	This work
$BaTiO_3$	Multilayer thick film	80	7.1	80	0.09	0.12		DSC	14
$BaTiO_3$	Multilayer thick film	80	1.8	17.6	0.10	0.26	2.1	DSC	22
Doped $BaTiO_3$	Ceramic multilayer ceramic capacitor (MLCC)	47	0.5	30	0.02	0.02	0.4	Direct	23
$Ba_{0.7}Sr_{0.3}TiO_3$	Ceramic MLCC	40	4.8	50	0.10			DSC	24
$BaZr_{0.2}Ti_{0.8}O_3$ (low field)	Ceramic	38	1.1	2.1	0.52	0.93	2.2	Direct	15
$BaZr_{0.2}Ti_{0.8}O_3$ (high field)	Ceramic	39	4.5	14.5	0.31	0.54	2.7	Direct	15
$BaTiO_3$	Ceramic	118	0.4	0.75	0.53			Direct	25
P(VDF-TrFE-CFE)[a]	Polymer	30	15.7	150	0.10	0.49	55.0	Direct	26
$BaTiO_3$	Single crystal	129	0.7	1.2	0.58	0.79	0.4	Direct	13
$Sr_{0.75}Ba_{0.25}Nb_2O_6$	Single crystal	80	0.4	1	0.4			DSC	27

[a]P(VDF-TrFE-CFE) refers to poly(vinylidenefluoride-trifluorethylene-chlorofluoroethylene).

the secondary effect, which contributes to the ECE. For some materials, the secondary effect can be comparable or even larger than primary effect. This may be the reason for the enhancement of EC effect in the BZT thick film in this work.

In summary, a giant ECE under room temperature is investigated in BZT thick film. Thick film is exerted with stress from the substrate and exhibits a large ΔT of 7.0 °C, large entropy change of 12.2 $J \cdot kg^{-1} \cdot K^{-1}$, and large EC coefficient ($\Delta T/\Delta E = 0.50 \times 10^{-6}$ $K \cdot m \cdot V^{-1}$ and $\Delta S/\Delta E = 0.88 \times 10^{-6}$ $J \cdot m \cdot kg^{-1} \cdot K^{-1} \cdot V^{-1}$) over 40 K temperature range near room temperature. These properties added together indicate a general solution of the EC materials with high performance for practical cooling applications.

Hui-Jian Ye acknowledges Ms. Amanda Baker for the help on the fabrication of BZT thick film. This work was supported by the Army Research Office under Grant No. W911NF-11-1-0534. D.-Y. Jeong thanks for the financial support from Inha University.

[1]M. E. Lines and A. M. Glass, *Principles and Applications of Ferroelectrics and Related Materials* (Clarendon, Oxford, 1977).
[2]T. Mitsui, I. Tatsuzaki, and E. Nakamura, *Introduction to the Physics of Ferroelectricity* (Gordon and Breach, London, 1976).
[3]Y. Sinyavsky and V. Brodyansky, Ferroelectrics **131**, 321 (1992).
[4]F. Jona and G. Shirane, *Ferroelectric Crystals* (Dover, New York, 1993).
[5]R. I. Epstein and K. J. Malloy, J. Appl. Phys. **106**, 064509 (2009).
[6]Y. Jia and Y. S. Ju, Appl. Phys. Lett. **100**, 242901 (2012).
[7]H. Gu, X. S. Qian, X. Li, B. Craven, W. Zhu, A. Cheng, S. C. Yao, and Q. M. Zhang, Appl. Phys. Lett. **102**, 122904 (2013).
[8]S. Kar-Narayan, S. Crossley, X. Moya, V. Kovacova, J. Abergel, A. Bontempi, N. Baier, E. Defay, and N. D. Mathur, Appl. Phys. Lett. **102**, 032903 (2013).
[9]A. S. Mischenko, Q. Zhang, J. F. Scott, R. W. Whatmore, and N. D. Mathur, Science **311**, 1270 (2006).
[10]B. Neese, B. Chu, S. G. Lu, Y. Wang, E. Furman, and Q. M. Zhang, Science **321**, 821 (2008).
[11]E. Defay, S. Crossley, S. Kar-Narayan, X. Moya, and N. D. Mathur, Adv. Mater. **25**, 3337 (2013).
[12]B. Rožič, M. Kosec, H. Uršič, J. Holc, B. Malič, Q. M. Zhang, R. Blinc, R. Pirc, and Z. Kutnjak, J. Appl. Phys. **110**, 064118 (2011).
[13]X. Moya, E. Stern-Taulats, S. Crossley, D. González-Alonso, S. Kar-Narayan, A. Planes, L. Mañosa, and N. D. Mathur, Adv. Mater. **25**, 1360 (2013).
[14]Y. Bai, G. P. Zheng, K. Ding, L. Qiao, S. Q. Shi, and D. Guo, J. Appl. Phys. **110**, 094103 (2011).
[15]X. S. Qian, H. J. Ye, Y. T. Zhang, H. Gu, X. Li, C. A. Randall, and Q. M. Zhang, Adv. Funct. Mater. **24**, 1300 (2014).
[16]X. S. Qian, S. G. Lu, X. Li, H. Gu, L. C. Chien, and Q. M. Zhang, Adv. Funct. Mater. **23**, 2894 (2013).
[17]Y. Bai, X. Han, X. C. Zheng, and L. Qiao, Sci. Rep. **3**, 2895 (2013).
[18]B. Peng, H. Fan, and Q. Zhang, Adv. Funct. Mater. **23**, 2987 (2013).
[19]Y. Liu, J. Wei, P.-E. Janolin, I. C. Infante, X. Lou, and B. Dkhil1, Appl. Phys. Lett. **104**, 162904 (2014).
[20]H. X. Cao and Z. Y. Li, J. Appl. Phys. **106**, 094104 (2009).
[21]G. Yang, Z. Yue, Z. Gui, and L. Li, J. Appl. Phys. **104**, 074115 (2008).
[22]Y. Bai, G. P. Zheng, and S. Q. Shi, Appl. Phys. Lett. **96**, 192902 (2010).
[23]S. Kar-Narayan and N. D. Mathur, J. Phys. D: Appl. Phys. **43**, 032002 (2010).
[24]K. Ding and G. P. Zhang, J. Electroceram. **32**, 169 (2014).
[25]A. I. Karchevskii, Sov. Phys. -Solid State **3**, 2249 (1962).
[26]X. Li, X. S. Qian, S. G. Lu, J. Cheng, Z. Fang, and Q. M. Zhang, Appl. Phys. Lett. **99**, 052907 (2011).
[27]F. L. Goupil, A. K. Axelsson, L. J. Dunne, M. Valant, G. Manos, T. Lukasiewicz, J. Dec, A. Berenov, and N. M. Alford, Adv. Energy Mater. **4**, 1301688 (2014).
[28]S. G. Lu and Q. M. Zhang, Adv. Mater. **21**, 1983 (2009).
[29]X. Moya, S. Kar-Narayan, and N. D. Mathur, Nat. Mater. **13**, 439 (2014).
[30]Z. K. Liu, X. Li, and Q. M. Zhang, Appl. Phys. Lett. **101**, 082904 (2012).
[31]X. Li, S. G. Lu, X. Z. Chen, H. Gu, X. S. Qian, and Q. M. Zhang, J. Mater. Chem. C **1**, 23 (2013).
[32]M. H. Lee, R. Guo, and A. S. Bhalla, J. Electroceram. **2**, 229 (1998).
[33]S. Lu, B. Rozic, Q. Zhang, Z. Kutnjak, and R. Pirc, Appl. Phys. A: Mater. Sci. Process. **107**, 559 (2012).